J Math Chem (2008) 44:731–742
DOI 10.1007/s10910-008-9350-2

ORIGINAL PAPER

# Comparative analysis of linear and nonlinear models for ion transport problem in chronoamperometry

**Alemdar Hasanov · Şafak Hasanoglu**

Received: 21 September 2007 / Accepted: 18 October 2007 / Published online: 1 February 2008


**Abstract** Ion transport problem related to controlled potential experiments in electrochemistry is studied. The problem is assumed to be superposition of diffusion and migration under the influence of an electric field. The comparative analysis are presented for three well-known models—pure diffusive (Cottrell's), linear diffusion-migration, and nonlinear diffusion-migration (Cohn's) models. The nonlinear model is derived by the identification problem for a nonlinear parabolic equation with nonlocal additional condition. This problem reduced to an initial-boundary value problem for nonlinear parabolic equation. The nonlinear finite difference approximation of this problem, with an appropriate iteration algorithm is derived. The comparative numerical analysis for all three models shows an influence of the nonlinear migration term, the valences of oxidized and reduced oxidized species, also diffusivity to the value of the total charge. The obtained results permits one to estimate bounds of linear and nonlinear ion transport models.

**Keywords** Ion transport · Cottrell's model · Cohn's model · Nonlinear parabolic problem · Current response · Iteration scheme

## 1 Introduction

In recent years there has been growth of interest in mathematical and computational modeling of electroanalytical experiments related to ion transport (see, [1–10] and

A. Hasanov (✉)
Department of Mathematics, Faculty Art and Sciences, Kocaeli University, Umuttepe Kampusu, Izmit, Kocaeli 41380, Turkey
e-mail: ahasanov@kou.edu.tr

Ş. Hasanoglu
Chemical-Engineering Division, Köseköy High School, Kocaeli University, Izmit, Kocaeli, Turkey

references therein). Linear mathematical models of such problems in electrochemistry, in general, and in chronoamperometry, in particular, are usually based on the Nernst–Planck equation [3]. Analytical solutions of these simplest models permit one to understand experiment, and to find out some relationships, which can not be estimated experimentally. In chronoamperometry such a classical result has first been obtained by Cottrell [4]. In 1902 Cottrell derived a linear initial-boundary value problem (IBVP) and demonstrated that, if an extreme potential is suddenly applied to an electrode in contact with a solution containing a uniform concentration of an electroreactant, then the resulting current response $\mathcal{I}_C$, defined to be as Cottrellian, is proportional to $1/\sqrt{t}$. Subsequently this result has also been confirmed experimentally and theoretically. This relationship assumes that the ion transport is purely diffusive, planar and semi-infinite. Deviations from the ideal Cottrellian response provide information about complex chemical kinetics and kinetics of electron transfer. Further various modifications of the relationship $\mathcal{I}_C \sim 1/\sqrt{t}$ were investigated based on linear mathematical models. Thus, the transport response of electrodes under conditions of diffusion and migration was studied by Lange and Doblhofer [5]. They used the Nernst–Planck equation to derive a linear model for the transport of the electroactive species with zero initial condition. The problem then was solved by digital simulation techniques. For equal diffusion coefficients of all ions a linear model with an analytical formula and some numerical results have been obtained by Myland and Oldham [6]. Here the effect of migration factor to the limiting Cottrell currents was also studied. For the case of unequal diffusion coefficients this linear model was developed by Bieniasz [7]. Here the effects of the diffusivity ratio $D_R/D_C$, as well as of the electroactive and counter-ions on the limiting chronoamperometric currents were examined. Analytical formulas of the current response, and comparative analysis for linear models in chronoamperometry under conditions of diffusion and migration, were given by Hasanov and Hasanoglu [8,9].

The mathematical model of mass and charge transport in a controlled potential experiment is derived by Cohn et al. [10]. Due to lack of electrochemical information, this model is restricted to the two-species (oxidized and reduced) case. However, even in this simplest, from the point of view physico-chemical model, case the obtained mathematical problem is highly complicated, as we will see below.

In the case of two-species migrating under the influence of the electric field, the scaled mathematical model with respect to the concentration $u(x,t)$ of the reduced species leads to the following identification problem for the nonlinear parabolic equation with the unknown coefficient $q(t)$ [10]:

$$\begin{cases} u_t = (g(u)u_x)_x + q'(t)h(u)_x, \quad x > 0, \quad t > 0, \\ u(x,0) = 0, \quad x > 0, \\ u(0,t) = 1, \quad t > 0, \end{cases} \tag{1}$$

and with the additional nonlocal condition

$$q(t) = \int_0^\infty u(x,t)dx, \quad t \geq 0. \tag{2}$$

The coefficients $g(u) > 0$ and $h(u)$ express an influence of the diffusion and migration in the ion transport and have the forms:

$$g(u) := \frac{z_o + (z_r - z_o)u}{z_o + (z_r\kappa - z_o)u}, \quad h(u) := \frac{\kappa u}{z_o + (z_r\kappa - z_o)u}. \tag{3}$$

Here $z_r$ and $z_o$ is the valences of the reduced and oxidized species, which are assumed to be integers of the same sign. The dimensionless parameter $\kappa := D_r/D_o$ is the diffusivity ratio.

Problem (1)–(2) can be regarded as a nonlocal identification problem with respect to the unknown coefficient $q(t)$, which represents the scaled total charge

$$q(t) = \frac{z_r}{n\mathcal{F}S_e u_0} Q(t). \tag{4}$$

Here $n$ is the number of electrons gained by an ion upon reduction, F is Faraday's constant, $S_e$ is the area surface of the electrode, and $u_0$ is the concentration at $x = 0$ of the reduced species at the electrode. The total charge carried by the reduced species is defined to be

$$Q(t) = \int_0^t \mathcal{I}(\tau)d\tau,$$

where $\mathcal{I}(t)$ is the current response. Exchange of electrons between the surface of the electrode and electroactive species in the time $t > 0$ gives rise to the *current response* $\mathcal{I} = \mathcal{I}(t)$, which is related to the concentration of reduced species by the balance equation [3]

$$\frac{u_0}{z_r}\int_0^\infty u(x,t)dx = \frac{1}{n\mathcal{F}S_e}\int_0^t \mathcal{I}(\tau)d\tau. \tag{5}$$

To our knowledge, the nonlinear model (1)–(2), interesting also from the point of view nonlocal inverse/optimal control problems, still is not neither analyzed mathematically, nor solved numerically. The only similarity solution of this problem is studied in [11–13]. Note that for the constant diffusion coefficient one special case of the problem (1)–(2) is considered in [14].

In this article we study the nonlinear mathematical model (1)–(2) related to ion transport in a polymeric medium under the influence of the electric field. Our study is aimed to estimate relationship between the linear and nonlinear models, and find out similarities and differences for these models. The presented results also show the degree of applicability of classical linear models.

In the next section the describe some important physico-chemical and mathematical aspects of the nonlinear model is derived. In Sect. 3 a method of reducing of the identification problem (8) to the initial-boundary value problem for nonlinear parabolic

equation is derived. An effective numerical algorithm for this problem is derived in Sect. 4. The comparative analysis of the linear and nonlinear models for ion transport problem is presented the Sect. 5. The final Sect. 6 contains some conclusions.

## 2 Some important physico-chemical and mathematical aspects of the nonlinear model

Although the mathematical model of the nonlinear ion transport problem is given in [10], for completeness, we briefly discuss here some distinguished features of the scaled model (1)–(2). The general background of the physico-chemical aspects of the problem can be found in [3,15].

Let $x \geq 0$ and $t \geq 0$ are the scaled space and time variables. To describe a standard experiment, we assume that there is an electrode at $x = 0$, and a polymeric medium containing mobile ions and electroactive species extending from the electrode to $x = \infty$. It is assumed that the electroactive species are in oxidized form before the time $t = 0$. At $t = 0$ a potential $E$ is introduced at the electrode. This causes a fraction of the oxidized species at the surface of the electrode to be reduced. We denote by $u = u(x, t)$, $D > 0$ and $c > 0$, the scaled concentration, diffusion and convection of the *reduced species*. As oxidized species are reduced at the surface of the electrode, its concentration decreases, and the concentration $u = u(x, t)$ of the reduced species at the electrode increases. As a result there arises two diffusion processes: oxidized species diffuse in toward $x = 0$, and the reduced species, out into the medium. Therefore ion transport here can be regarded as a superposition of *diffusion*, which is the random motion of small particles immerse in the medium, *migration*, which is a motion under the influence of an electric field, and *convection*, which is a hydrodynamic flow. Exchange of electrons between the surface of the electrode and electroactive species in the time $t > 0$ gives rise to the *current response* $\mathcal{I} = \mathcal{I}(t)$, which is related to the concentration of reduced species by the balance equation (5).

Considering the mathematical model (1)–(2) of the identification problem we will only assume that the following relationship $z_r D_r = z_o D_o$ holds between the valences and diffusivities $D_r$ and $D_o$ of the reduced and oxidizes species. Note that the valences $z_r$, $z_o$ are assumed to be integers of the same sign, and $z_r \neq -1$, $z_o \neq 1$, since one electron must be gained in reduction. In practice, $-4 < z_r < z_o \leq -1$ and $1 < z_r < z_o \leq 3$. Within the above assumption the values of valences and the diffusivity ratio $\kappa := D_r/D_o$ are given in Table 1.

Under this assumption the second nonlinear term $h(u)_x$ in the parabolic equation (1) becomes $h(u)_x := u/z_r$. Hence the functions $g(u)$ and $h(u)$, defined by (3), have the following forms:

**Table 1** The values of valences and the diffusivity ratio

| $z_o$ | $-1$ | $-2$ | $-3$ | 2 | 3 |
|---|---|---|---|---|---|
| $z_r$ | $-2$ | $-3$ | $-4$ | 1 | 2 |
| $\kappa := D_r/D_o$ | 1/2 | 2/3 | 3/4 | 2 | 3/2 |

$$g(u) := 1 + \left(\frac{z_r}{z_o} - 1\right)u, \quad h(u) := \frac{1}{z_r}u. \tag{6}$$

Although the assumption $z_r D_r = z_o D_o$ makes some restrictions, it still permits one to analyze the nonlinear model (1)–(2) for real class of materials.

Further, experimental and theoretical results show that [10] for a fixed $t \in (0, \infty)$ the function $u(x, t)$ and its partial derivative $u_x(x, t)$ decreases rapidly to zero, as $x \to \infty$, i.e.

$$u(1, t) = u_x(1, t) = 0, \quad t > 0. \tag{7}$$

Moreover, the values of the function $u(x, t)$ are in $[0, 1]$, i.e. $0 \leq u(x, t) \leq 1$, $\forall x > 0, \quad t > 0$.

Taking into account the above properties, the nonlinear model (1)–(2) can be reformulated in the bounded parabolic domain $\Omega_T := (0, l) \times (0, T]$ as follows:

$$\begin{cases} u_t = ((1 + (1/\kappa - 1)u)u_x)_x + \frac{1}{z_r}q'(t)u_x, \quad (x, t) \in \Omega_T, \\ u(x, 0) = 0, \quad x \in (0, 1), \\ u(0, t) = 1, \quad u_x(0, t) = 0, \quad t > 0, \\ q(t) = \int_0^\infty u(x, t)dx, \quad t \geq 0. \end{cases} \tag{8}$$

In sequel this model will be considered as a basic nonlinear model.

## 3 Reducing of the identification problem (8) to the nonlinear initial-boundary value problem

In this section we are going to reduce the identification problem (8) to the initial-boundary value problem for nonlinear parabolic equation, eliminating the nonlocal additional condition (2).

Differentiating the both sides of (2) and using then the parabolic equation (8) we get:

$$q'(t) = \int_0^l (g(u)u_x)_x dx + \frac{1}{z_r}q'(t)\int_0^l u_x dx.$$

Integrating the right hand side terms yields:

$$q'(t) = g(u(l, t))u_x(l, t) - g(u(0, t))u_x(0, t) - \frac{1}{z_r}q'(t)[u(l, t) - u(0, t)].$$

Using here the conditions $u(l, t) = u_x(l, t) = 0$, also, $g(u(0, t)) = g(1) = 1/\kappa$, we get

$$q'(t) = -\frac{1}{\kappa}u_x(0, t) - \frac{1}{z_r}q'(t).$$

Therefore

$$q'(t) = -\frac{z_r}{(1+z_r)\kappa} u_x(0,t), \tag{9}$$

and

$$q(t) = -\frac{z_r}{(1+z_r)\kappa} \int_0^t u_x(0,\tau)d\tau, \quad t \in [0,T]. \tag{10}$$

Note that this approach has also been used in [10] to estimate the derivatives $u_x$ and $u_{xx}$, and founders on some difficulties. We will use this approach to reduce the identification problem (12)–(13) eliminating the coefficient $q(t)$, in order to construct the numerical algorithm. Further this approach will be used also to formulate a fixed-point principle.

Substituting (9) in the parabolic equation (8) we obtain

$$\begin{cases} u_t = (g(u)u_x)_x - \frac{1}{(1+z_r)\kappa} u_x(0,t)u_x, \quad (x,t) \in \Omega_T; \\ u(x,0) = 0, \quad x \in (0,l); \\ u(0,t) = 1, \ \ u_x(l,t) = 0, \quad t \in (0,T]. \end{cases} \tag{11}$$

Therefore, the nonlinear identification problem (8) is reduced to the initial-boundary value problem (11) for the strongly nonlinear parabolic equation $u_t = (g(u)u_x)_x - (1/(1+z_r)\kappa)u_x(0,t)u_x$. This problem does not contain the unknown function $q(t)$. The main distinguished feature of this approach is that the problem of solving the identification problem (8) is separated into the two subproblem: solving the nonlinear parabolic problem (11) and finding the unknown function $q(t)$ by the integration formula (2).

Formula (10) shows that the scaled total charge $q(t)$ can also be expressed the total flux $(1/\kappa)u_x(0,t)$ at the left boundary $x = 0$, over the time $[0,t]$. This, with the balance equation (5) means that, the current response $\mathcal{I}(t)$ can me measured via the flux at the left boundary $x = 0$:

$$\mathcal{I}(t) = -\frac{n\mathcal{F}S_e u_0}{(1+z_r)\kappa} u_x(0,t).$$

## 4 The finite-difference approximation and the iteration algorithm

We derive here an iteration algorithm for the reduced problem (11), using an implicit finite difference scheme for nonlinear parabolic equations [16]. In the presented iteration algorithm, the values of the coefficients in the diffusion and migration terms in the nonlinear parabolic equation is be taken from the previous iteration. This mean that the nonlinear problem (11) is linearized as follows:

$$\begin{cases} u_t^{(n)} = (g(u^{(n-1)})u_x^{(n)})_x - \frac{1}{(1+z_r)\kappa} u_x^{(n-1)}(0,t)u_x^{(n)}, \quad (x,t) \in \Omega_T; \\ u^{(n)}(x,0) = 0, \quad x \in (0,l); \\ u^{(n)}(0,t) = 1, \ \ u_x^{(n)}(l,t) = 0, \quad t \in (0,T], \end{cases} \tag{12}$$

where the parameter $n = 1, 2, 3, \ldots$ shows the number of iterations.

To approximate the linearized problem (12), we define the uniform space and time meshes $w_h = x_i \in (0,l] : x_i = ih_x; \ h_x = l/N, w_\tau = t_j \in (0,T] : t_j = j\tau; \ h_t = T/M$, and use the standard finite difference approximations [16]

$$u_{x,ij} := \frac{u_{i+1,j} - u_{i,j}}{h_x}, \ \ u_{t,ij} := \frac{u_{i,j+1} - u_{i,j}}{h_t}, \ \ u_{i,j} := u(x_i, t_j), \ i = \overline{1, N}, \\ j = \overline{1, M}$$

of the partial derivatives $\partial u/\partial x$, $\partial u/\partial t$. Here the constants $h_x$ and $h_t$ are the mesh steps.

For the numerical solution of the linearized problem (12) the following implicit finite difference scheme is used [16]:

$$\begin{cases} \frac{u_{i,j+1}^{(n)} - u_{i,j}}{h_t} - \frac{1}{h_x}\left[ g\left(u_{i+1/2,j}^{(n-1)}\right) \frac{u_{i+1,j+1}^{(n)} - u_{i,j+1}^{(n)}}{h_x} - g\left(u_{i-1/2,j}^{(n-1)}\right) \frac{u_{i,j+1}^{(n)} - u_{i-1,j+1}^{(n)}}{h_x} \right] \\ + \frac{z_r}{(1+z_r)\kappa} \frac{u_{2,j+1}^{(n-1)} - u_{1,j+1}^{(n-1)}}{h_x} \frac{u_{i+1,j+1}^{(n)} - u_{i-1,j+1}^{(n)}}{2h_x} = 0, \ \ i = \overline{1, N-1}, \ \ j = \overline{2, M}; \\ u_{i,1} = 0, \ \ i = \overline{1, N} \\ u_{1,j} = 1, \ \frac{u_{N,j+1} - u_{N-1,j+1}}{h_x} = 0, \ \ j = \overline{2, M}. \end{cases} \tag{13}$$

To analyze the convergence and accuracy of the discrete model (13) consider the following test example.

The analytical solution of the reduced problem

$$\begin{cases} u_t = (g(u)u_x)_x - (1/(1+z_r)\kappa)\, u_x(0,t)u_x + F(x,t), \quad (x,t) \in \Omega_T; \\ u(x,0) = 0, \quad x \in (0,l); \\ u(0,t) = t, \ \ u_x(l,t) = 0, \quad t \in (0,T], \end{cases} \tag{14}$$

with non-homogeneous source term

$$F(x,t) = \cos(\pi x) - \left(\frac{1}{\kappa} - 1\right) \pi^2 t^2 \sin^2(\pi x) \\ + \left[1 + \left(\frac{1}{\kappa} - 1\right) t \cos(\pi x)\right] \pi^2 t \cos(\pi x),$$

is the function $u(x,t) = t\cos(\pi x)$. Note that here the Dirichlet data in the boundary condition $u(0,t) = t$ depends on time.

**Table 2** Absolute sup-norm errors for different values of valences

| $z_o$ | $z_r$ | Abs. error |
|---|---|---|
| −2 | −3 | $4.5 \times 10^{-2}$ |
| −3 | −4 | $2.9 \times 10^{-2}$ |
| 2 | 1 | $3.6 \times 10^{-2}$ |
| 3 | 2 | $2.6 \times 10^{-2}$ |

The iteration scheme (13) is applied to the nonlinear problem (11) by using the mesh size $40 \times 40$ in the domain $(0, 1) \times (0, 1)$ which means $h_x = h_t = 2.5 \times 10^{-2}$. For different values of the valences $z_o$ and $z_r$ the absolute sup-norm difference $\varepsilon_h^{(n)}$, between the numerical solution $u_h^{(n)}$ and the function $u(x, t) = t \cos(\pi x)$ are shown in Table 2. The number of iterations for this accuracy is $n = 4$. As it is seen from the table, in all cases the absolute sup-norm error $\varepsilon_h^{(n)} = \max_{(ij)} |u - u_h^{(n)}|$ is of the order $\varepsilon_h^{(n)} = O(10^{-2})$.

These results show that the accuracy of discrete model (13) is high enough.

To study the behavior of the concentration function $u(x, t)$ with respect to the time $t > 0$ and space $x > 0$ variables, the computational experiments were done for different admissible values $z_o$ and $z_r$ of the valences of the oxidized and reduced species. For this aim the nonlinear problem (11) was solved by the iteration algorithm (13), with the functions $g(u)$ and $h(u)$, given by (6). For the values $\langle z_o, z_r \rangle = \langle -2, \ -3 \rangle$; $\langle -3, \ -4 \rangle$; $\langle 2, \ 1 \rangle$; $\langle 3, \ 2 \rangle$ of valences the numerical solutions $u_h^{(n)}$ are plotted in Fig. 1. As shown in all figures, for fixed time $t > 0$ the solution $u_h^{(n)}(x, t)$ decreases rapidly and monotonically on the space interval [0, 1]. Further, in all cases $u(x, t)$ is a smooth function. These results agree with the theoretical results obtained in [10], as well as with the experimental results described in [3,17]. Figure 1 also show that the behavior of the concentration function $u(x, t)$ with respect to the time variable $t > 0$ is different. Specifically, for fixed space variable $x > 0$, the solution $u_h^{(n)}(x, t)$ increases slowly and monotonically from 0 to 1 in the time interval [0, 1].

## 5 Comparative analysis between linear and nonlinear models

To derive the comparative analysis between linear models and the above nonlinear model for ion transport, first of all one need to find an upper and lower estimates for the nonlinear model (11) via the linear models. Without loss of generality, let us consider the case $\langle z_r, z_o \rangle = \langle -1, -2 \rangle$. Then $\kappa = z_o/z_r = 1/2$, and the coefficients $g(u)$ and $h(u)$, given by (6), have the following forms:

$$g(u) = 1 + u, \quad h(u) = -\frac{1}{2}.$$

Hence, the reduced parabolic equation (11) has the following form

$$u_t = ((1 + u)u_x)_x + 2u_x(0, t)u_x, \quad (x, t) \in \Omega_T. \tag{15}$$

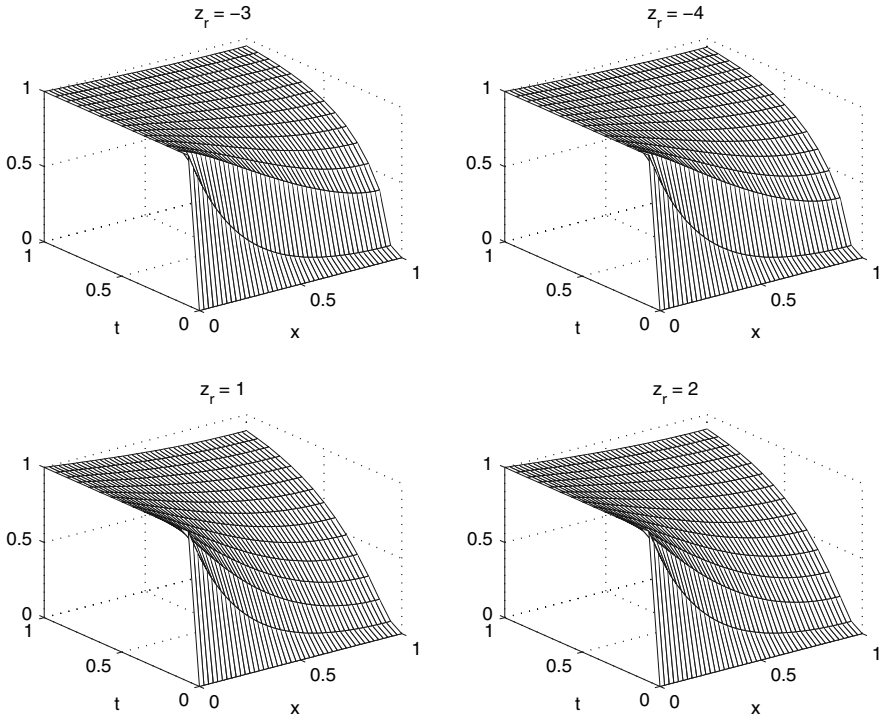


**Fig. 1** The numerical solution $u_h^{(n)}$ of the nonlinear problem (11) different values $z_o$ and $z_o$ of the valences of the oxidized and reduced species

Since the function $u(x,t)$ is a decreasing one with respect to the variables $x$ and $t$, the function $v(t) = -2u_x(0,t) > 0$ is a positive one. Further, $0 \le u(x,t) \le 1$ implies $D_* = 1 \le u(x,t) \le 2 = D^*$. Hence the linear models

$$\begin{cases} v_t = D_* v_{xx} - v(t)v_x, \quad (x,t) \in \Omega_T, \\ v(x,0) = 0, \quad x \in (0,l), \\ v(0,t) = 1, \quad v_x(l,t) = 0, \quad t \in (0,T]; \end{cases} \tag{16}$$

and

$$\begin{cases} w_t = D^* w_{xx} - v(t)w_x, \quad (x,t) \in \Omega_T, \\ w(x,0) = 0, \quad x \in (0,l), \\ w(0,t) = 1, \quad w_x(l,t) = 0, \quad t \in (0,T], \end{cases} \tag{17}$$

with $D_* = 1$ and $D^* = 2$, can be considered as the upper and lower linear models, respectively, for the nonlinear model (11), when $\langle z_r, z_o \rangle = \langle -1, -2 \rangle$. For $v(t) = 0$ these models represent pure diffusive models.

On the other hand the analytical formula (see, [8], formula (5))

$$\mathcal{I}_C(t) = \frac{n\mathcal{F}S_e u_0}{z_r}\sqrt{\frac{D}{\pi t}} \tag{18}$$

for the classical Cottrellian $\mathcal{I}_C$ holds for the pure diffusive model in the half-space domain $\Omega_+ = (x,t) \in R^2 : x > 0, \;\; t > 0$. This means that the analytical formula

$$q(t) = 2\sqrt{\frac{D}{\pi}t} \tag{19}$$

for the scaled total charge holds for the linear model

$$\begin{cases} u_t = Du_{xx} - \nu(t)u_x, & (x,t) \in \Omega_+, \\ w(x,0) = 0, & x > 0, \\ w(0,t) = 1, & t > 0, \end{cases} \tag{20}$$

given on the half-space domain $\Omega_+ = (x,t) \in R^2 : x > 0, \;\; t > 0$, but not for the linear model (16) (or (17)), with $\nu(t) = 0$, given on the bounded domain $\Omega_T = (x,t) \in R^2 : x \in (0,1) > 0, \;\; t \in (0,T]$. Hence, to derive the comparative analysis, first of all, one needs to compare the values the scaled total charge $q(t)$, obtained by the above linear models, in the case of pure diffusivity (with $\nu(t) = 0$). For this aim the linear problems (16) and (17), with $D_* = 1$, $D^* = 2$, and $\nu(t) = 0$, were solved numerically, and the scaled total charge $q(t)$ was calculated by the formula (2). Then, for the same values $D_* = 1$ and $D^* = 2$ of the diffusion coefficient the scaled total charge $q(t)$ was calculated by the formula (19), which corresponds to the linear model (20), with $\nu(t) = 0$. The results are plotted in Fig. 2. These results show that for a small time scales the values of the scaled total charge $q(t)$ obtained by the linear models, given in half-space domain $\Omega_+$ and the bounded domain $\Omega_T$, are close. However, for increasing values of the time $t > 0$ these values become highly different. Hence, even in the case of pure diffusion linear model, the classical Cottrellian $\mathcal{I}_C(t)$ can only qualitatively reflect the current response. This means that for real physical problems one needs to consider these models in the finite domain $\Omega_T$.

To compare the upper and lower linear models (16)–(17) with the corresponding nonlinear model, problem (11), with the nonlinear equation $u_t = ((1+u)u_x)_x$, was solved by the above iteration algorithm, for the given data $\langle z_r, z_o \rangle = \langle -1, -2 \rangle$. The scaled total charge $q(t)$, corresponding to the nonlinear model is plotted by the dashed-line (- - -) in Fig. 2. It is seen that the values of the function $q(t)$ are between the values of the scaled total charge obtained by the upper and lower linear models (16)–(17). This shows that the linear models can also be used as an upper and lower estimations for the total charge, as well as for the current response.

The second series of computational experiments is related to the behavior of the scaled total charge $q(t)$ depending on the values $\langle z_o, z_r \rangle$ of valences of the oxidized and reduced species. The nonlinear problem (11) with the given in (6) coefficients is solved for the given in Table 2 negative and positive values of valences. The corresponding total charges, calculated by formula (2), are plotted in Fig. 3. For the negative

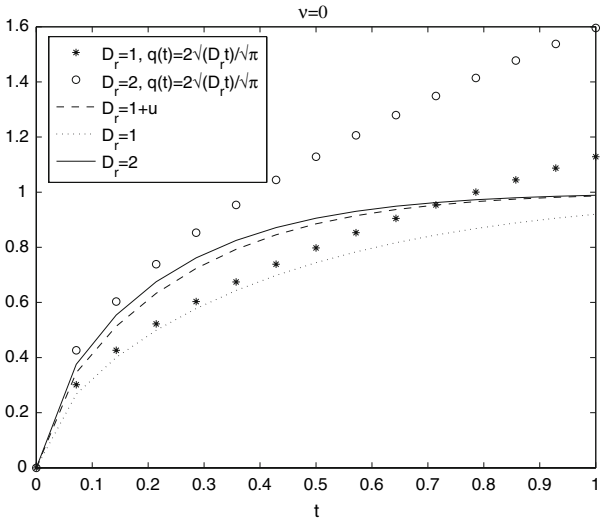


**Fig. 2** The scaled total charge $q(t)$ corresponding to the linear pure diffusive models (16), (17), (20), and obtained from the nonlinear model (11) with $\langle z_r, z_o\rangle = \langle -1, -2\rangle$

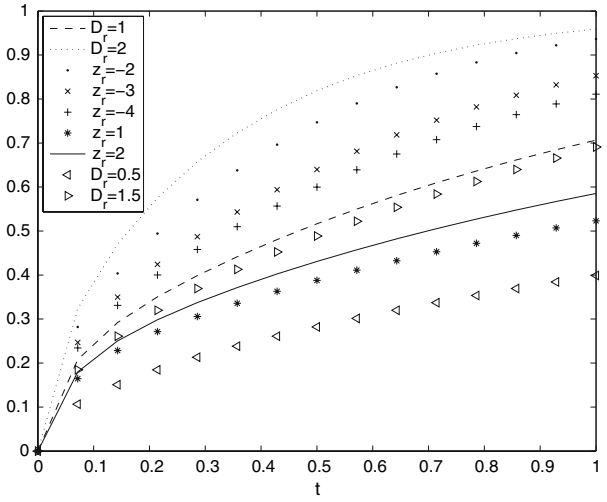


**Fig. 3** The scaled total charge $q(t)$ corresponding to the linear pure diffusive upper and lower models (16)–(17), and obtained from the nonlinear model (11) for the admissible values of valences of the oxidized and reduced species

three values ($\langle z_o, z_r\rangle = \langle -1, \ -2\rangle, \langle -2, \ -3\rangle; \langle -3, \ -4\rangle$) of valences the diffusion coefficient $g(u)$ is estimated as follows: $D_* = 1 \leq g(u) \leq D^* = 2$. Hence linear models (16)–(17) with these diffusivity coefficients $D_* = 1$ and $D^* = 2$ play rule of the upper and lower ones. Figure 3 clearly shows that in all three cases the values of the scaled total charge $q(t)$ are between the values of the scaled total charge obtained by the upper and lower linear models (16)–(17). The same situation can be

observed for two positive values $\langle z_o, z_r \rangle = \langle 2,\ 1 \rangle; \langle 3,\ 2 \rangle$ of valences. In this case $D_* = 0.5 \leq g(u) \leq D^* = 1.5$.

## 6 Conclusions

In this article, we performed a comparative analysis of the linear and nonlinear mathematical models related to ion transport. For this aim we reduce the identification problem (1)–(2) to the initial-boundary value problem for nonlinear parabolic equation, and propose an effective iteration algorithm for the numerical solution of this problem. Our first comparative analysis between the existing linear models show the deviation of the classical Cottrellian $\mathcal{I}_C(t)$ from the real current response. The second comparative analysis between the linear and nonlinear models show how can be obtained upper and lower bounds for the scaled total charge, corresponding to the nonlinear model, via the appropriate upper and lower linear models.

**Acknowledgements** The author is grateful to Arzu Erdem for the assistance in providing the computational experiments. The research has been supported by INTAS through the international research project (Grant No. 06-1000017-8909), and by the Scientific and Technological Research Council of Turkey (TUBITAK)

## References

1. M. Ciszkowska, Z. Stojek, J. Electroanal. Chem. **466**, 129 (1999)
2. W. Kucza, M. Danielewski, A. Lewenstam, Electrochem. Commun. **8**, 416 (2002)
3. A.J. Bard, L.R. Faulkner, Electrochemical Methods (Wiley, New York, 1980)
4. F.G. Cottrell, Z. Phys. Chem. **42**, 385 (1903)
5. R. Lange, K. Doblhofer, J. Electroanal. Chem. **237**, 13 (1987)
6. J.C. Myland, K.B. Oldham, Electrochem. Commun. **1**, 467 (1999)
7. L.K. Bieniasz, Electrochem. Commun. **4**, 917 (2002)
8. A. Hasanov, Şafak Hasanoglu, Math. Chem. 10 (2007) (to appear)
9. A. Hasanov, Şafak Hasanoglu, Math. Chem. (2008) (to appear)
10. S. Cohn, K. Pfabe, J. Redepenning, Math. Mod. Meth. Appl. Sci. **9**, 455 (1999)
11. A. Hasanov, Math. Meth. Appl. Sci. **21**, 1195 (1998)
12. A. Hasanov, J.L. Mueller, S. Cohn, J. Redepenning, Comput. Math. Appl. **39**, 225 (2000)
13. K. Pfabe, T.S. Shores, Appl. Numer. Math. **32**, 175 (2000)
14. Şafak Hasanoglu, Arzu Erdem, Math. Chem. 10 (2008) (to appear)
15. L. Liberti, F.G. Helffrich, Mass Transfer and the Kinetics of Ion Exchange (NATO ASI Series) (Martinus Mijhoff, Boston, 1987)
16. A.A. Samarskii, The Theory of Difference Schemes (Marcel Dekker, New York, 2001)
17. R.P. Buck, M.B. Madaras, R. Mäckel, Diffusion-migration capacitance in homogeneous membranes, modified electrodes and thin-layer cells. J. Electroanal. Chem. **366**, 55–68 (1994)